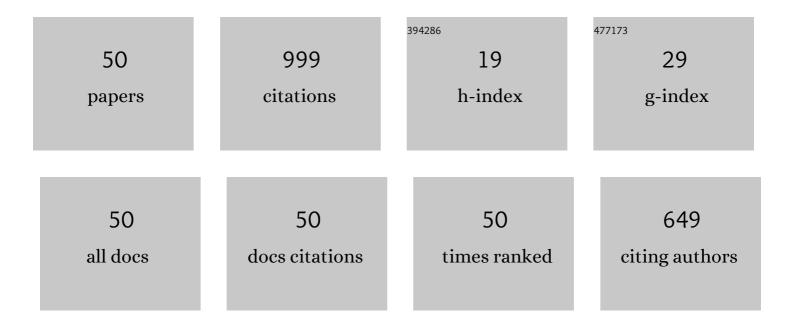
## Bin Leng

## List of Publications by Year in descending order

Source: https://exaly.com/author-pdf/3758406/publications.pdf Version: 2024-02-01



RINLENC

#	Article	IF	CITATIONS
1	Effect of yttrium content on the corrosion behavior of nickel-based UNS N10003 alloy in high-temperature molten LiF-NaF-KF salt. Corrosion Science, 2022, 194, 109940.	3.0	5
2	Tellurium segregation-induced intergranular corrosion of GH3535 alloys in molten salt. Corrosion Science, 2022, 194, 109944.	3.0	13
3	Highâ€ŧemperature corrosion behavior of Inconel 617 with Ni laddings in molten FLiNaK salt. Materials and Corrosion - Werkstoffe Und Korrosion, 2022, 73, 486-496.	0.8	2
4	Corrosion behaviors of Ni-WC cemented carbide in high temperature molten fluoride salt and vapor. Journal of Nuclear Materials, 2022, 561, 153541.	1.3	4
5	Metallic impurities induced corrosion of a Ni-26W-6Cr alloy in molten fluoride salts at 850 oC. Corrosion Science, 2021, 178, 109079.	3.0	14
6	Effect of Isothermal Aging on Microstructure Evolution of Ni Claddings on Inconel 617. Journal of Materials Engineering and Performance, 2021, 30, 2389-2398.	1.2	5
7	Effect of SO42â^' ion impurity on stress corrosion behavior of Ni-16Mo-7Cr alloy in FLiNaK salt. Journal of Nuclear Materials, 2021, 547, 152809.	1.3	8
8	Corrosion behavior of carburized 316 stainless steel in molten chloride salts. Solar Energy, 2021, 223, 1-10.	2.9	17
9	Effect of high temperature molten salt corrosion on the microstructure of a Co-Mo-Cr-Si wear resistant alloy. Materials Characterization, 2021, 179, 111377.	1.9	8
10	Effect of thermal aging on corrosion behavior of type 316H stainless steel in molten chloride salt. Corrosion Science, 2021, 191, 109784.	3.0	20
11	Unexpected accelerated corrosion of Cr in Ni-xW-6Cr alloy with W content increasing. Corrosion Science, 2021, 191, 109761.	3.0	6
12	Non-uniform corrosion of UNS N10003 alloy induced by trace SO42- in molten FLiNaK salt. Corrosion Science, 2021, 192, 109802.	3.0	6
13	Corrosion behavior of a wear resistant Co-Mo-Cr-Si alloy in molten fluoride salts. Journal of Nuclear Materials, 2020, 542, 152529.	1.3	12
14	Effect of grain boundary carbides on the diffusion behavior of Te in Ni-16Mo-7Cr base superalloy. Materials Characterization, 2020, 164, 110329.	1.9	8
15	Effect of graphite particles in molten LiF-NaF-KF eutectic salt on corrosion behaviour of GH3535 alloy. Corrosion Science, 2020, 168, 108581.	3.0	13
16	On the possibility of severe corrosion of a Ni-W-Cr alloy in fluoride molten salts at high temperature. Corrosion Science, 2019, 149, 218-225.	3.0	42
17	Effect of Surface Decarburization on Corrosion Behavior of GH3535 Alloy in Molten Fluoride Salts. Acta Metallurgica Sinica (English Letters), 2019, 32, 401-412.	1.5	4
18	Effects of post-weld heat treatment on microstructure and mechanical properties of Hastelloy N superalloy welds. Materials Today Communications, 2019, 19, 230-237.	0.9	14

Bin Leng

#	Article	IF	CITATIONS
19	Influence of grain size on tellurium corrosion behaviors of GH3535 alloy. Corrosion Science, 2019, 148, 110-122.	3.0	29
20	Corrosion of Incoloy 800H alloys with nickel cladding in FLiNaK salts at 850â€Â°C. Corrosion Science, 2018, 133, 349-357.	3.0	50
21	Effect of SO42â^' on the corrosion of 316L stainless steel in molten FLiNaK salt. Corrosion Science, 2018, 144, 224-229.	3.0	46
22	Effect of thermal exposure time on tellurium-induced embrittlement of Ni–16Mo–7Cr–4Fe alloy. Nuclear Science and Techniques/Hewuli, 2017, 28, 1.	1.3	14
23	Effect of Cr contents on the diffusion behavior of Te in Ni-based alloy. Journal of Nuclear Materials, 2017, 497, 101-106.	1.3	25
24	Grain boundary engineering for control of tellurium diffusion in GH3535 alloy. Journal of Nuclear Materials, 2017, 497, 76-83.	1.3	20
25	R&D of Structural Alloy for Molten Salt Reactor in China. , 2016, , .		1
26	The tensile behavior of GH3535 superalloy at elevated temperature. Materials Chemistry and Physics, 2016, 182, 22-31.	2.0	55
27	M 2 C and M 6 C carbide precipitation in Ni-Mo-Cr based superalloys containing silicon. Materials and Design, 2016, 112, 300-308.	3.3	47
28	Effect of long-term thermal exposure on the hot ductility behavior of GH3535 alloy. Materials Science & Engineering A: Structural Materials: Properties, Microstructure and Processing, 2016, 673, 299-306.	2.6	15
29	Intermediate temperature embrittlement of one new Ni-26W-6Cr based superalloy for molten salt reactors. Materials Science & Engineering A: Structural Materials: Properties, Microstructure and Processing, 2016, 668, 137-145.	2.6	34
30	STEM-EDS analysis of fission products in neutron-irradiated TRISO fuel particles from AGR-1 experiment. Journal of Nuclear Materials, 2016, 475, 62-70.	1.3	10
31	Effects of post-weld heat treatment on microstructure and mechanical properties of laser welds in GH3535 superalloy. Optics and Laser Technology, 2016, 81, 18-25.	2.2	23
32	Effect of tungsten content on the microstructure and tensile properties of Ni–xW–6Cr alloys. Materials Science & Engineering A: Structural Materials: Properties, Microstructure and Processing, 2016, 655, 269-276.	2.6	29
33	Effect of carbon ion irradiation on Ag diffusion in SiC. Journal of Nuclear Materials, 2016, 471, 220-232.	1.3	11
34	EPMA and TEM characterization of intergranular tellurium corrosion of Ni–16Mo–7Cr–4Fe superalloy. Corrosion Science, 2015, 97, 1-6.	3.0	30
35	Observations of Ag diffusion in ion implanted SiC. Journal of Nuclear Materials, 2015, 461, 314-324.	1.3	17
36	Intergranular diffusion and embrittlement of a Ni–16Mo–7Cr alloy in Te vapor environment. Journal of Nuclear Materials, 2015, 467, 341-348.	1.3	18

Bin Leng

#	Article	IF	CITATIONS
37	Corrosion behavior of an alumina forming austenitic steel exposed to supercritical carbon dioxide. Corrosion Science, 2014, 82, 67-76.	3.0	79
38	Grain boundary sliding at high temperature deformation in cold-rolled ODS ferritic steels. Journal of Nuclear Materials, 2014, 452, 628-632.	1.3	21
39	Hot-rolling of reduced activation 8CrODS ferritic steel. Journal of Nuclear Materials, 2013, 443, 59-65.	1.3	1
40	Effect of hot-rolling and cooling rate on microstructure and high-temperature strength in 9CrODS steel. Journal of Nuclear Materials, 2013, 440, 553-556.	1.3	5
41	Characterization of recrystallization of 12Cr and 15Cr ODS ferritic steels. Journal of Nuclear Science and Technology, 2013, 50, 314-320.	0.7	18
42	Grain Boundary Related Deformation in ODS Ferritic Steel during Creep Test. Materials Transactions, 2012, 53, 1753-1757.	0.4	15
43	Hardness and Micro-Texture in Friction Stir Welds of a Nanostructured Oxide Dispersion Strengthened Ferritic Steel. Materials Transactions, 2012, 53, 390-394.	0.4	19
44	Effects of Two-Step Cold Rolling on Recrystallization Behaviors in ODS Ferritic Steel. Materials Transactions, 2012, 53, 652-657.	0.4	19
45	Oxide Particle Refinement in 4.5 mass%Al Ni-Based ODS Superalloys. Materials Transactions, 2012, 53, 645-651.	0.4	24
46	Recrystallization Texture of Cold-rolled Oxide Dispersion Strengthened Ferritic Steel. ISIJ International, 2011, 51, 951-957.	0.6	26
47	Grain Boundary Deformation at High Temperature Tensile Tests in ODS Ferritic Steel. ISIJ International, 2011, 51, 982-986.	0.6	16
48	Directional recrystallization of ODS alloys by means of zone annealing. Journal of Nuclear Materials, 2011, 417, 171-175.	1.3	13
49	Grain characteristic and texture evolution in friction stir welds of nanostructured oxide dispersion strengthened ferritic steel. Science and Technology of Welding and Joining, 2011, 16, 690-696.	1.5	24
50	Refinement of Oxide Particles by Addition of Hf in Ni-0.5 mass%Al-1 mass%Y <sub>2</sub> O <sub>3</sub> Alloys. Materials Transactions, 2010, 51, 2019-2024.	0.4	44